The isotope effect on the geodesic acoustic mode spatial structure and its interaction with small-scale turbulence in the FT-2 tokamak

A.D. Gurchenko[1,2], E.Z. Gusakov[1,2], A.B. Altukhov[1,2], L.A. Esipov[1,2], M.Yu. Kantor[1,2], D.V. Kouprienko[1,2], S.I. Lashkul[1,2], A.A. Perevalov[1,2]

[1] *Ioffe Institute, St. Petersburg, Russia*

[2] *St. Petersburg State Polytechnical University, RLPAT, St. Petersburg, Russia*

Geodesic acoustic modes (GAMs) and low-frequency zonal flows are considered nowadays as features of micro-turbulence induced self-control [1]. According to analytical results and numerical modelling this control occurs in two ways. Firstly, GAMs are driven by the turbulent Reynolds stress in an energy conserving process so that their generation necessarily corresponds to a reduction of drift-wave energy. Secondly, shearing of the drift-waves by GAMs possessing finite wavelength, as a result of three-wave-interaction, nonlinearly transfers energy to smaller radial scales where it is linearly dissipated. Because of this important role last decade GAM was in focus of experimental studies utilizing different diagnostic techniques. The highly localised correlative Doppler upper hybrid resonance (UHR) backscattering (BS) technique capable of simultaneous measurements of GAM and small-scale turbulence [2] opens further options for studying their interplay and detailed investigation of the GAM spatial structure.

According to the theoretical expectations [3] the radial structure of the GAM potential, localised near the cutoff position r_0, is described by Airy function: $\varphi = \mathrm{Ai}\left((r_0 - r)/\lambda_{\mathrm{Ai}}\right)$, where $\lambda_{\mathrm{Ai}} = \rho_i^{2/3} L_T^{1/3}$, ρ_i is an ion gyroradius and L_T is the temperature gradient scale length. The GAM wavelength should take the maximal value dependent on the ion mass equal to $\lambda_G = 4\lambda_{\mathrm{Ai}}$ near the point r_0. The expected isotope effect on the GAM spatial structure and its interaction with small-scale turbulence is investigated in this paper.

The Doppler UHR BS technique is applied at the small-size FT-2 tokamak. The UHR BS technique [4] utilizes *X*-mode microwave plasma probing out of the tokamak's equatorial plane from the high magnetic field side. In this geometry the diagnostic is benefiting from the growth of electric field and poloidal wave number in the UHR $k_{\mathrm{iUHR}\theta}$, resulting in enhanced scattering signal, sub-mm radial resolution and substantially increased Doppler frequency shift $2\pi f_D = 2k_{\mathrm{iUHR}\theta} V_\theta = \kappa_\theta V_\theta$, where κ_θ is the poloidal wave number of the fluctuation leading to BS and V_θ is its poloidal phase velocity. The dual frequency

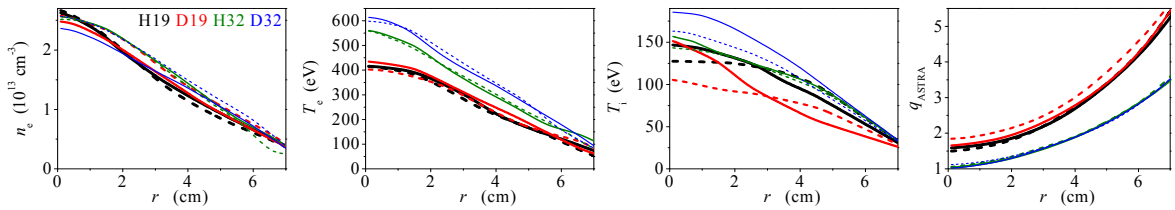

Fig. 1. *Profiles of main parameters in four regimes (solid* – 27 ms*, dashed* – 36 ms*, r – flux surface radius).*

measurements accompanied by correlation analysis provides the small-scale turbulence wave number (κ_r, κ_θ) spectra and GAM wavelength and correlation length [2].

The measurements were carried out at FT-2 tokamak (R = 55 cm; a = 7.9 cm) in similar regimes with hydrogen or deuterium at two plasma currents 19 kA and 32 kA at toroidal magnetic field 2.3 T. The approximations of experimentally measured profiles used in ASTRA modeling are shown in fig. 1, together with the safety factor q reconstruction.

Profiles of the contrast (power-to-noise ratio) of the spectral line dominating in the $f_D(t)$ signal which is associated with poloidal velocity GAM component is shown in fig. 2 together with line's frequency F for all four regimes. The isotope effect leads to expected down shift of the GAM frequency in deuterium regimes in comparison with hydrogen. The same effect was quantitatively investigated in [2] for 19 kA regimes where comparison with theoretical estimations for GAM frequency [5] was done. Another effect is the larger level of the GAM line's contrast observable in deuterium. The effective electron thermal diffusivity $\chi_{eff} = -q_{eff} / (n \nabla T_e)$, where q_{eff} is the total (diffusive plus convective) electron heat flux, is shown in fig. 2 at the bottom. The local correlation of the lower level of the GAM contrast with a higher value of χ_{eff} is seen not only from the comparison of two different times in each regime, but also in comparison of the H and D discharges.

The radial GAM structure was investigated at r = 4.8-5.2 cm with dual frequency probing correlative scheme providing two f_D signals from two spatially separated UHR regions [2]. The corresponding coherence spectra and dependencies of cross-phases φ vie Δr at GAM frequency are shown in fig. 3 by circles. The slope of the linear part of φ(Δr) provides the

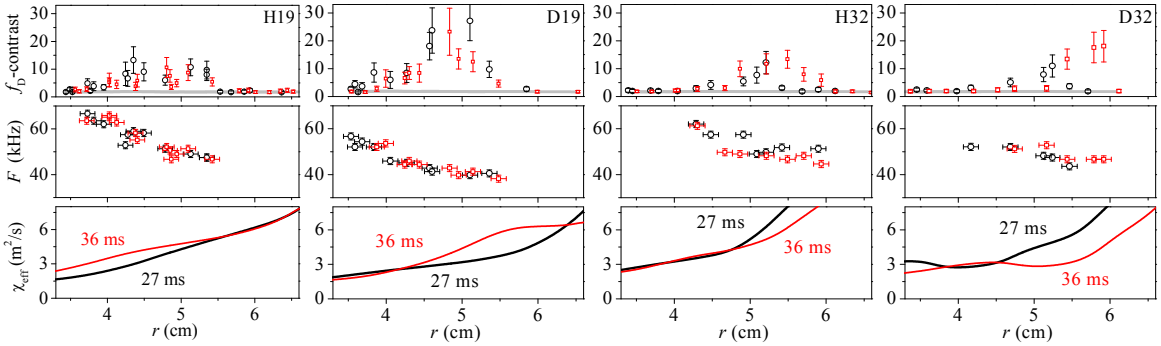

Fig. 2. *GAM contrast (grey line - f_D noise), GAM frequency and χ_{eff} (t* = 27 ms - *black and* 36 ms - *red).*

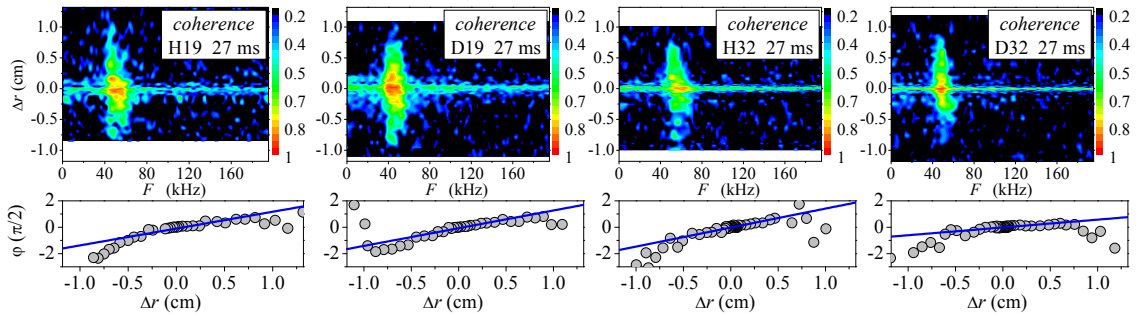

Fig. 3. *The coherence and cross-phase between two f_D signals at $r \approx 5$ cm ($\Delta r > 0$ – outward direction).*

estimation of the GAM radial wave length λ_r and phase velocity V_r plotted in fig. 4 together with the radial correlation length l_{cr}. The comparison of λ_r with λ_G is shown on right side in fig. 4. Experimentally measured wave length significantly exceeds the maximal value predicted in theory [3].

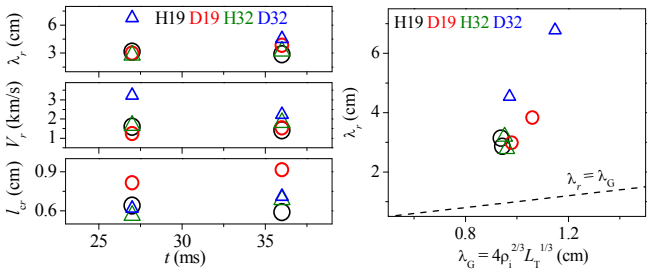

Fig. 4. *GAM properties and comparison of λ_r and λ_G.*

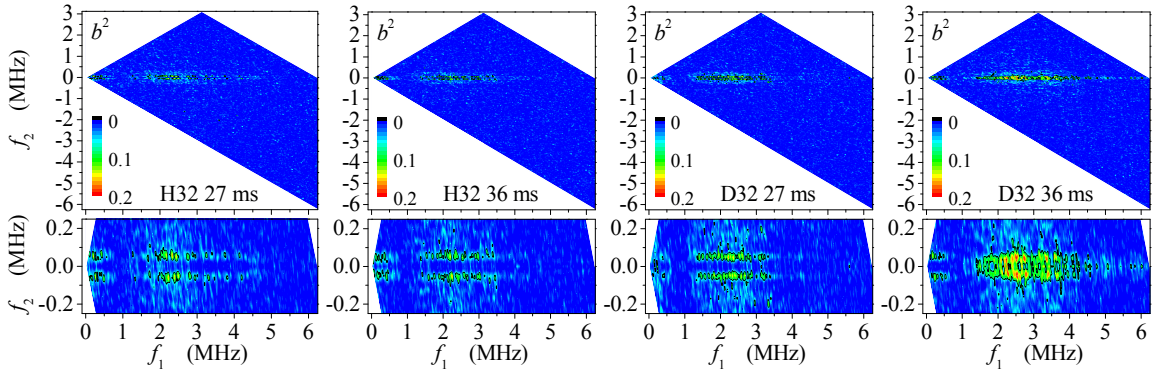

Fig. 5. *Cross-bicoherence spectra measured at $r \approx 5$ cm in* H32 *and* D32 *regimes.*

An evidence for a GAM interaction with plasma turbulence via three-wave coupling was obtained by the bicoherency analysis. The cross-bicoherence spectra $b^2(f_1, f_2) = \left|\left\langle A(f_1) f_D(f_2) A^*(f_1 \pm f_2)\right\rangle\right|^2 \Big/ \left(\left\langle \left|A(f_1) f_D(f_2)\right|^2 \right\rangle \left\langle \left|A(f_1 \pm f_2)\right|^2 \right\rangle\right)$, where $A(f_1)$, $A(f_2)$ and $A(f_1 \pm f_2)$ are harmonics of the complex Fourier spectrum of the UHR BS signal, which are proportional to density fluctuations at the same frequency, $f_D(f_2)$ and $f_D(f_1 \pm f_2)$ are harmonics of the $f_D(t)$ spectrum, are shown in fig. 5 and demonstrate the weak interaction of GAM with HF (2-4 MHz) turbulence. The UHR BS signals' spectra corresponding to these cases are shown in fig. 6 and the intermittency of GAM was taken into account during the κ-spectra reconstruction procedure by selection of time intervals where GAMs are excited or suppressed. The turbulence has a slightly larger level when analysed during intervals where GAM is suppressed, but the shape of the turbulence κ-

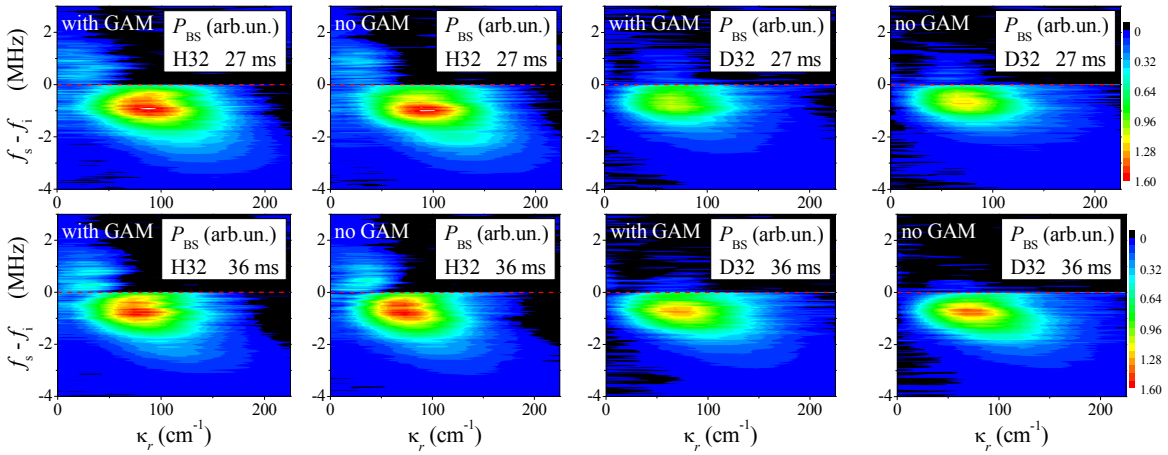

Fig. 6. *UHR BS spectra calculated in* H32 *and* D32 *regimes for realizations with and without GAM at* $r \approx 5$ cm *(f_i = 64.4 GHz – probing, f_s – scattered frequency).*

spectra shown in fig. 7 does not change much. It should be also mentioned that the comparison of H32 and D32 cases reveals the difference between HF turbulence κ-spectra which correlates with enhancement of the b^2 spectrum in D32 regime. Namely, as it is seen in fig. 5, κ_r-spectra in the case of higher bicoherency are characterised by a slower decay.

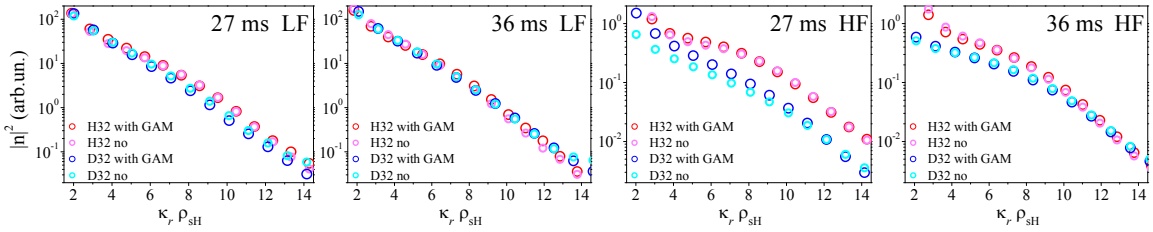

Fig. 7. *Turbulence spectra reconstructed in* H32 *and* D32 *regimes for realizations with and without GAM for* LF (-1.9; 0 MHz) *and* HF (-4; -1.9 MHz) *UHR BS signal's bands at* $r \approx 5$ cm, where $\rho_{sH} = \rho_{iH} T_e^{0.5}/(2T_i)^{0.5}$.

In summary, we would like to underline a big excess of the observed GAM radial wave length over that predicted theoretically [3], which can be interpreted in favor of observation of GAMs nonlinearly induced by drift-wave turbulence rather than those which freely propagate in plasma. The anticorrelation of GAM and the electron thermal diffusivity behavior both spatial and temporal provides an argument in favor of their role in transport phenomena in FT-2.

Financial support of RFBR grant 13-02-00614, the Russian Academy Presidium program №12, the RF Government grant 11.G34.31.0041, NWO-RFBR Centre-of-Excellence grant 047.018.002 is acknowledged.

[1] P.H. Diamond, S.-I. Itoh, K. Itoh and T.S. Hahm 2005 *PPCF* **47** R35
[2] A.D. Gurchenko, Gusakov E.Z., Altukhov A.B. et al. 2013 *PPCF* **55** 085017
[3] K. Itoh, S.-I. Itoh, P.H. Diamond et al. 2006 *Plasma Fusion Res.* **1** 037
[4] E.Z. Gusakov, A.D. Gurchenko, A.B. Altukhov et al. 2006 *PPCF* **48** A371
[5] W. Guo, S. Wang and J. Li 2010 *Phys. Plasmas* **17** 112510